

# Photoreduction of Flavin by NADH. A Flash Photolysis Photo-CIDNP Study

P. J. Hore, A. Volbeda, K. Dijkstra, and R. Kaptein\*

Contribution from the Department of Physical Chemistry, University of Groningen, Nijenborgh 16, 9747 AG Groningen, The Netherlands. Received March 8, 1982

**Abstract:** A 360-MHz  $^1\text{H}$  CIDNP investigation of the photoreaction of  $\beta$ -NADH (nicotinamide adenine dinucleotide) with a substituted lumiflavin (7,8,10-trimethyl-3-carboxymethylisoalloxazine) has been performed with the recent technique of laser flash photolysis NMR. Nuclear spin polarization is observed in both NADH itself and the reaction product,  $\text{NAD}^+$ . In the presence of oxygen, CIDNP spectra are consistent with a primary electron-transfer step from NADH to triplet-state flavin. Back electron transfer within the geminate radical ion pair generates polarized NADH, while the escaping  $\text{NADH}^+$  cation radicals deprotonate and react with dissolved oxygen to give  $\text{NAD}^+$ . The lack of CIDNP time dependence during the period 1  $\mu\text{s}$ –100 ms after flash photolysis agrees with this oxidation being diffusion controlled. In oxygen-free solution, however, the  $\text{NAD}^+$  polarization is seen, by comparison with INDO calculated hyperfine coupling constants, to be characteristic of the neutral radical  $\text{NAD}\cdot$ . CIDNP results show that  $\text{NADH}^+$  is an oxidant while  $\text{NAD}\cdot$  is a reductant toward flavosemiquinone radicals. The slow time dependence of the  $\text{NAD}^+$  polarization found in degassed solution probably reflects the slow oxidation of  $\text{NAD}\cdot$  by residual oxygen of flavin. CIDNP spectrum simulations of the strong multiplet effect seen for the C-4 methylene protons in NADH gives information on the hyperfine couplings and  $g$  value of  $\text{NADH}^+$ .

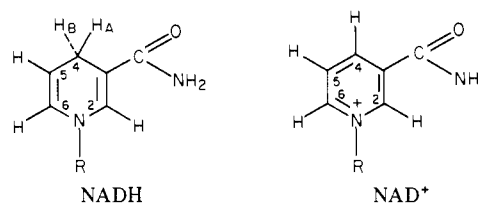
## I. Introduction

Current interest in nicotinamide-derived radicals stems from the possibility of one-electron pathways in NAD(P)H-mediated enzymatic redox reactions.<sup>1</sup> In dehydrogenases the transfer of the C-4 hydrogen is stereospecific and involves no exchange with solvent. H/D kinetic isotope effects in enzymatic and model reactions vary between 2 and 6.<sup>2</sup> These facts, however, are inconclusive as to the question of one- vs. two-electron transfer.<sup>2c</sup> Probably, depending on the substrate and reaction conditions, both hydride transfer and radical pair formation can occur in reactions of 1,4-dihydronicotinamides.

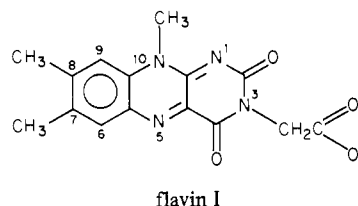
The NADH-flavin (or flavoprotein) redox couple is important in the respiratory electron transport chain. Studies with model flavins have shown that charge-transfer complexes are formed.<sup>1c</sup> Again, these may further lead to either single electron-transfer intermediates<sup>1c,d</sup> or hydride transfer,<sup>2b</sup> a question that has not yet been settled.

In photochemical reactions of NADH model compounds, electron-transfer processes seem to be predominant. Thus, photoexcited 1-benzyl-1,4-dihydronicotinamide (BNAH) is known to be quenched via a one-electron transfer process by a variety of electron acceptors.<sup>3</sup> The photomediated reduction of olefins by BNAH also proceeds via electron transfer as the first step.<sup>4</sup> However, a study<sup>5</sup> of the photoreduction of riboflavin and 5-deazaflavin by NADH was inconclusive as to the mechanism of the primary step although direct hydrogen transfer was favored.

In this paper we report a CIDNP study of the photochemical reaction of 7,8,10-trimethyl-3-carboxymethylisoalloxazine (flavin I, F) with NADH which has led to insight into the reaction mechanism as well as to be characterization of potentially important NADH derived radical intermediates.



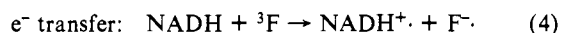
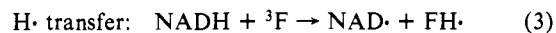
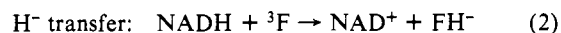
R = adenosine-diphosphoribosyl



The net reaction of NADH with a flavin may be written:



where  $\text{FH}_2$  is the reduced form of the flavin. Assuming that the excited triplet state of the flavin is the reactive species, there are three possibilities for the primary step after light absorption and intersystem crossing:



$\text{FH}\cdot$  and  $\text{F}\cdot$  are neutral and anionic flavosemiquinones, respectively. In each case the initial step would be followed by secondary reactions and/or (de)protonations to yield the final products,  $\text{NAD}^+$  and  $\text{FH}_2$ .

It should be realized that the photoreaction and the thermal enzymatic reaction may not proceed by the same mechanism and that from a CIDNP study alone it is difficult to assess the importance of photoreactions proceeding by nonradical pathways, for example, reaction 2.

Most of this work was performed on  $\beta$ -NADH; for comparison photo-CIDNP spectra were also measured for its anomer,  $\alpha$ -NADH, and for nicotinamide mononucleotide, NMNH. For convenience in what follows the name NADH will be taken to imply the  $\beta$  form.

To investigate these reactions the recently developed technique of laser flash photolysis nuclear magnetic resonance spectroscopy

(1) For reviews see: (a) Kill, R. J.; Widdowson, D. A. In "Bioorganic Chemistry"; van Tamelen, E. E., Ed.; Academic Press: New York, 1978; Vol. IV, p 239. (b) Sigman, D. S.; Hajdu, J.; Creighton, D. J. *Ibid.* p 385. (c) Kosower, E. M. In "Free Radicals in Biology"; Pryor, W. A., Ed.; Academic Press: New York, 1976; Vol. II, p 1. (d) Bruce, T. C. In "Progress in Bioorganic Chemistry"; Kaiser, F. T., Kezdy, F. J., Eds.; Wiley: New York, 1976; Vol. IV, p 1.

(2) (a) Klinman, J. P. *Biochemistry* 1976, 15, 2018. (b) Blankenhorn, G. *Eur. J. Biochem.* 1976, 67, 67. (c) Kurz, L. C.; Kurz, J. L. *Ibid.* 1978, 90, 283.

(3) (a) Martens, F. M.; Verhoeven, J. W.; Gase, R. A.; Pandit, U. K.; De Boer, Th. J. *Tetrahedron* 1978, 34, 443. (b) Martens, F. M.; Verhoeven, J. W. *Recl. Trav. Chim. Pays-Bas* 1981, 100, 228.

(4) Pac, C.; Ihama, M.; Yasuda, M.; Miyachi, Y.; Sakurai, H. *J. Am. Chem. Soc.* 1981, 103, 6495.

(5) Sun, M.; Song, P. S. *Biochemistry* 1973, 12, 4663.

py<sup>6-10</sup> has been employed. Just as conventional flash photolysis methods with UV/visible detection are widely used to follow the progress of photochemical processes, so this technique provides "time-resolved" NMR spectra at given delays after a photolytic flash.

The experiment proceeds thus: a sample in the probe of an NMR spectrometer is subjected to a short laser flash followed, after a preset delay, by a radiofrequency (rf) pulse with flip angle  $\leq 90^\circ$ . The resulting free induction decay (FID) is then recorded. This sequence can be repeated if necessary to improve signal-to-noise with coaddition of the FIDs. Subsequent Fourier transformation gives a time-resolved NMR spectrum with line intensities proportional to the spin-state population differences at the time the rf detection pulse was applied. Repetition of this procedure at different delays between light and rf pulses reveals the time evolution of the spectrum. If reaction products exhibit nuclear polarization, considerable spectral simplification can be achieved by using difference<sup>10</sup> or presaturation<sup>6</sup> methods to remove all unpolarized lines.

At present, time-resolved NMR is restricted to studying processes occurring on time scales longer than 0.1–1.0  $\mu$ s, the limiting factor being the duration of acceptable rf pulses.<sup>9</sup> The development of high-power pulse amplifiers and modifications in probe design should improve this situation. However, even with this rather low time resolution (by the standards of UV flash photolysis), one can investigate a variety of chemical and physical events, taking advantage of the spectral resolution of high-field NMR. Applications to date include the kinetics of triplet states and biradicals,<sup>8</sup> the separation of geminate and F-pair CIDNP effects,<sup>6</sup> and the CIDNP time dependence resulting from cyclic reactions, in which reactants and products are identical.<sup>10</sup> In the last case, cancellation of opposite phase recombination and escape-type polarizations can occur giving indirect information on the kinetics of the reactions responsible.

The above experiment and its ESR counterparts<sup>11</sup> are to some extent complementary. With the latter, one observes the paramagnetic intermediates of chemical reactions, whereas the NMR method is most usefully applied to their diamagnetic reactants and products. If CIDNP effects are present, however, the NMR spectrum contains information on the magnetic properties, kinetics, and reaction pathways of free radicals, a fact which is exploited below. NMR often has the advantage over ESR of more straightforward spectral assignment and hence greater ease of identification of reaction intermediates or products.

Advantages of flash photolysis photo-CIDNP over more familiar experiments using lamps or CW lasers<sup>12,13</sup> include the lack of intensity distortions from spin relaxation and to some extent freedom from the cancellation effects alluded to above.

## II. Experimental Section

<sup>1</sup>H NMR measurements were performed at 360 MHz on a Bruker HX-360 spectrometer equipped with an Aspect 2000 computer. The flash photolysis NMR method as described elsewhere<sup>10</sup> was used with the following alterations. To improve time resolution, modifications were made to the NMR probe: the height of the rf gap was reduced by 40% and the tuning capacitors moved closer to it to minimize losses. In this way the 90° pulse length was reduced to 5  $\mu$ s and pulses as short as 1  $\mu$ s could be obtained with minimal distortion or phase instability. In place of the difference method<sup>10</sup> for suppressing unpolarized peaks the entire spectrum was saturated immediately prior to the light flash. This was achieved by a train of 90° pulses separated by variable delays, each



Figure 1. (A) NMR spectrum of 2 mM  $\beta$ -NADH + 0.2 mM flavin I in D<sub>2</sub>O, pH 7.0, 50 mM phosphate buffer (KD<sub>2</sub>PO<sub>4</sub>), several minutes after laser irradiation. (B) Photo-CIDNP spectrum of NADH + flavin I (same conditions as (A)) 10- $\mu$ s delay after a single laser flash; 5- $\mu$ s rf pulse. Assignments of the polarized lines are indicated. (C) Fourfold expansion of part of (B). (D) Computer simulation of the NADH + NAD<sup>+</sup> CIDNP spectrum using  $A(2) = 1.0$  G,  $A(4a) = 46.8$  G,  $A(4b) = 45.8$  G,  $A(5) = -6.2$  G,  $A(6) = 1.5$  G,  $A(1') = 5$  G,  $\Delta g = -0.0002$ .

delay being approximately half the preceding one. This gave not only the anticipated<sup>14</sup>  $\sqrt{2}$  improvement in signal to noise but also much better suppression of large peaks. To obtain further reduction of the HDO solvent, line gated decoupling was performed in some experiments during the above pulse sequence.

The light source was a Phase-R 2100B dye laser operating with  $5 \times 10^{-5}$  M coumarin 504 (Exciton Chemical Co.) in methanol (Uvasol, Merck) containing 1% by volume amonox LO (Lambda Physik). It produced 3-J light flashes of 0.5- $\mu$ s duration in the wavelength range 484–537 nm with maximum intensity at 499 nm.

In all experiments, satisfactory results could be obtained with a single laser flash so that signal averaging was not necessary. The spectra used for extraction of hyperfine couplings and  $g$  values were recorded with short rf pulses (flip angle  $\sim 10^\circ$ ) to avoid distortion of multiplet CIDNP effects.<sup>14</sup>

Flavin I was the generous gift of Dr. F. Müller (Wageningen);  $\beta$ -NADH,  $\alpha$ -NADH, and NMNH (Sigma Chemical Co.) were used as supplied. All solutions were made up in 99.75% D<sub>2</sub>O. To avoid complications from the slow thermal reduction of flavin by NADH, stock solutions were mixed immediately prior to recording photo-CIDNP spectra. All measurements were made at room temperature, and chemical shifts are quoted with respect to DSS (sodium 2,2-dimethyl-2-silapentane-5-sulfonate).

## III. Photo-CIDNP Experiments

Figure 1 (B and C) shows the photo-CIDNP spectrum of NADH in the presence of flavin I 10  $\mu$ s after a single laser flash. A conventional NMR spectrum of the same sample, recorded after all polarization had relaxed, is included (Figure 1A). As indicated, polarized signals from both NADH and NAD<sup>+</sup> are observed together with a strong polarization of the HDO resonance. To check that the latter is not an artifact arising from incomplete suppression of the strong background signal, the experiment was repeated without a light flash. No NMR signals were observed confirming that the HDO polarization is indeed genuine.

(6) Closs, G. L.; Miller, R. J. *J. Am. Chem. Soc.* **1979**, *101*, 1639.  
 (7) Closs, G. L.; Sitzmann, E. V. *J. Am. Chem. Soc.* **1981**, *103*, 3217.  
 (8) Closs, G. L.; Miller, R. J. *J. Am. Chem. Soc.* **1981**, *103*, 3586.  
 (9) Miller, R. J.; Closs, G. L. *Rev. Sci. Instrum.* **1981**, *52*, 1876.  
 (10) Hore, P. J.; Zwieterweg, E. R. P.; Kaptein, R.; Dijkstra, K. *Chem. Phys. Lett.* **1981**, *83*, 376.  
 (11) For example: (a) Trifunac, A. D.; Norris, J. R.; Lawler, R. G. *J. Chem. Phys.* **1979**, *71*, 4380. (b) Fessenden, R. W.; Hornak, J. P.; Venkataraman, B. *Ibid.* **1981**, *74*, 3694. (c) Thirup, G.; Frykjaer, S. *J. Phys. E* **1980**, *13*, 1214. (d) Hore, P. J.; McLauchlan, K. A. *Mol. Phys.* **1981**, *42*, 1009.  
 (12) Muus, L. T.; Atkins, P. W.; McLauchlan, K. A.; Pedersen, J. B., Eds. "Chemically Induced Magnetic Polarization"; Reidel: Dordrecht, 1977.  
 (13) Kaptein, R. In "NMR Spectroscopy in Molecular Biology"; Pullman, B., Ed.; Reidel: Dordrecht, 1978; p 211.

(14) Schäublin, S.; Wokaun, S.; Ernst, R. R. *J. Magn. Reson.* **1977**, *27*, 273.

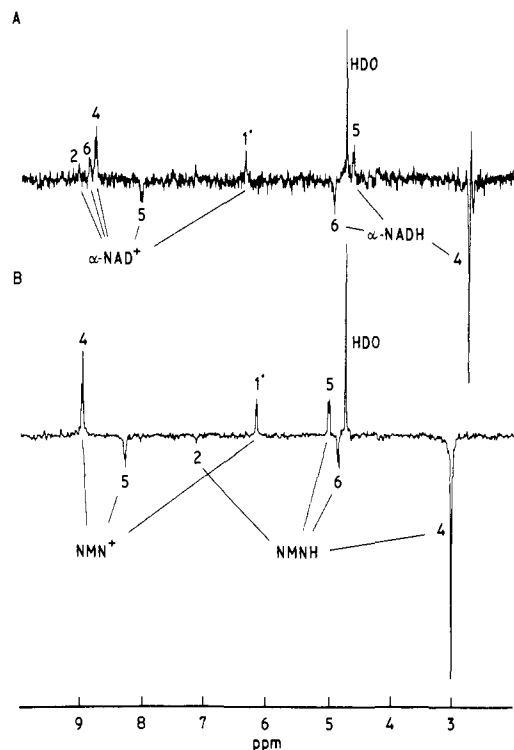


**Figure 2.** Photo-CIDNP spectra of (A) 2 mM  $\alpha$ -NADH and (B) 2 mM NMNH, with 0.2 mM flavin I in  $D_2O$ , pH 7.0, 50 mM  $KD_2PO_4$ , 10- $\mu$ s delay, 1 scan, 5- $\mu$ s rf pulse.

In NADH, the doublets at 2.63 and 2.85 ppm arising from the two nonequivalent C-4 protons exhibit a pronounced absorption-emission (A/E) multiplet effect superimposed on a smaller net emission. In addition to the C-2 and C-5 protons are weakly E and A polarized, respectively.  $NAD^+$  shows a net A polarization for its single C-4 proton and smaller effects for the C-2 (A), C-5 (E), C-6 (A), and C-1' ribose (A) protons. Also shown in Figure 1D is a computer simulation of the experimental spectrum which will be discussed in section VI.

For comparison the photo-CIDNP spectra of  $\alpha$ -NADH and NMNH solutions are presented in Figures 2A and 2B, respectively. Both are similar to that of  $\beta$ -NADH apart from the C-5 and C-6 proton resonances of the reduced forms which are here shifted clear of the HDO signal. NMNH, lacking the adenosine moiety, has equivalent C-4 protons and an emissive singlet at 3.02 ppm.

In these systems polarizations of the C-1' ribose proton was always detected in the oxidized but never in the reduced form of the nucleotides.

Returning to the  $\beta$ -NADH spectrum, Figure 1B, one can discriminate between the two primary radical producing steps, eq 3 and 4, on the basis of the observed polarization patterns. The only possible source of the C-4 protons' multiplet effect is a geminate recombination from a primary radical pair involving  $NADH^+$ . No such effect would be expected from the radical pair formed by C-4 H abstraction ( $NAD\cdot FH\cdot$ ) for the following reason. The abstracted hydrogen in  $FH\cdot$ , being attached to either N or O, should be rapidly exchanged in the presence of 50 mM phosphate buffer for a deuterium before transfer back to  $NAD\cdot$ . Under these circumstances, the remaining C-4 proton of NADH should exhibit only a net emissive polarization. Similarly, the generation of CIDNP by longer lived  $NADH^+$  radicals (via F radical pairs) can also be ruled out. The  $pK_a$  of this cation radical has been reported<sup>3b</sup> as -4 so that in phosphate buffered  $D_2O$  solution at pH 7 deprotonation would occur (although not as rapidly as in  $FH\cdot$ ), resulting once again in replacement with a deuterium. In addition, the large multiplet effect observed for NADH suggests a radical-pair precursor in which the two protons involved have large hyperfine couplings, which is the case for  $NADH^+ F\cdot$  but not for  $NAD\cdot FH\cdot$  (see section IV). Thus the

**Table I.** Proton Hyperfine Coupling Constants (in Gauss) of Nicotinamide Radicals Calculated by the INDO Method

radical <sup>a</sup>	A(2)	A(4a)	A(4b)	A(5)	A(6)	A(1')
$NAD\cdot$	-5.0	-8.8		3.0	-8.0	0-7 <sup>b</sup>
$NADH^+$	2.6	46	46	-6.2	2.0	0-21 <sup>b</sup>

<sup>a</sup> INDO calculations were carried out for 1-*N*-methylnicotinamide radicals on the basis of coordinates from X-ray data on the parent compounds  $NAD^+$  and  $NADH$ .<sup>17</sup> <sup>b</sup> Depending on the orientation of C-1' proton bond with respect to the nicotinamide ring.

NADH polarization must arise predominantly from the back-electron-transfer step:



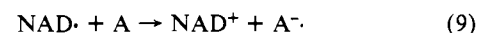
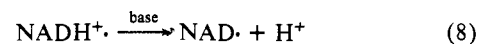
occurring  $10^{-9}$ - $10^{-8}$  s after formation of radicals according to reaction 4. As the initial step very probably proceeds via the triplet state of the flavin, the A/E multiplet effect together with the CIDNP sign rule:<sup>15</sup>

$$\Gamma_{mc}(a,b) = \mu\epsilon A_a A_b J_{ab} \sigma = + + + + - + = - (A/E) \quad (6)$$

indicates that step 5 populates the singlet state of the reaction partners, while the net-effect rule<sup>15</sup> implies that the *g* value of the  $NADH^+$  radical cation is smaller than that of the flavo-semiquinone:

$$\Gamma_{nc}(a) = \mu\epsilon A_a(\Delta g) = + + + - = - (E) \quad (7)$$

The  $NAD^+$  enhancements are opposite in phase to those of the corresponding protons in NADH and indicate an "escape" product. Most probably they arise from deprotonation of the  $NADH^+$  radicals escaping from the primary pair followed by electron transfer to a suitable acceptor which for the moment we shall call A:



The polarized  $H^+$  ion from  $NADH^+$  ends up in the water pool and is observed as an enhanced absorption for HDO (Figure 1B).

Measurements performed with a beam-chopped argon laser as light source reveal little dependence of the polarization intensities on the concentration of phosphate buffer up to 1 M at pH 8. On the CIDNP time scale ( $10^{-9}$ - $10^{-8}$  s), therefore, the  $NADH^+$  radical cation remains protonated (otherwise no multiplet effect would be observed). This puts an upper limit on the second-order rate constant for reaction 8 with phosphate ion as the base ( $k < 10^9 M^{-1} s^{-1}$ ), which is distinctly slower than diffusion controlled, not unusual for a carbon protonated radical.

#### IV. INDO Calculations

Before proceeding to a description of the observed CIDNP time dependence, it is useful to present the results of INDO calculations<sup>16</sup> on 1-*N*-methylnicotinamide radicals, as models for  $NADH^+$  and  $NAD\cdot$  (Table I). Important points to note are the large hyperfine couplings (hfc) of the C-4 protons in the radical cation (cf. 47.71 G for the analogous methylene protons in cyclohexadienyl<sup>18</sup>) and, with the exception of  $A(1')$ , the opposite signs of the hfc of corresponding protons in neutral and cationic radicals.

Comparison with Figure 1 shows broad agreement between the calculated hfc for  $NADH^+$  and the phase and amplitude of the CIDNP enhancements: a large hfc corresponding to a large enhancement.

(15) Kaptein, R. *Chem. Commun.* **1971**, 732.

(16) Pople, J. A.; Beveridge, D. L. "Approximate Molecular Orbital Theory"; McGraw-Hill: New York, 1970.

(17) (a) Koyama, H. *Z. Kristallografiya* **1963**, *118*, 51. (b) Voet, D. J. *J. Am. Chem. Soc.* **1973**, *95*, 3763.

(18) Fessenden, R. W.; Schuler, R. H. *J. Chem. Phys.* **1963**, *39*, 2147.

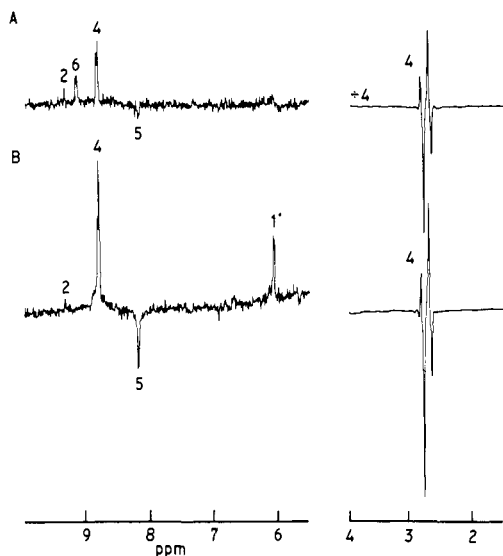


Figure 3. Photo-CIDNP spectra of  $\beta$ -NADH + flavin I in  $D_2O$ , 1- $\mu$ s delay in (A)  $N_2$ -saturated solution and (B)  $O_2$ -saturated solution (other conditions as for Figure 1B).

### V. CIDNP Time Dependence

As described in section I, further insight into the mechanism of the flavin/NADH photoreaction is available from the change in CIDNP intensities following a photolytic flash.

In nondegassed  $D_2O$  solutions no time dependence of the CIDNP signals was observed within experimental error during the period 1  $\mu$ s–100 ms after flash photolysis. Since flavin is a possible candidate for the electron acceptor in eq 9, its concentration might influence the rate of  $NAD^+$  production. In an attempt to detect this reaction, which would be much slower than the formation of polarized NADH by eq 5, the flavin concentration was kept as low as possible consistent with adequate signal to noise in the CIDNP spectrum. Even with 0.1 mM flavin using 2- $\mu$ s rf pulses, no CIDNP time dependence could be observed.

Different behavior was found in the absence of oxygen. Solutions of NADH and phosphate in  $D_2O$  were degassed by bubbling nitrogen through for 20 min; a small quantity of concentrated flavin solution was then added and a photo-CIDNP spectrum recorded immediately. In this way the thermal reaction was minimized. At 1- $\mu$ s delay the spectrum shown in Figure 3A was recorded: a number of differences from Figure 1B are noticeable. Firstly, all the  $NAD^+$  signals are weaker with respect to the NADH C-4 multiplet. Moreover, the relative intensities of the  $NAD^+$  resonances have changed: with respect to the C-4 signal, C-2 and C-6 are stronger and C-5 is weaker than in oxygenated solution, and the C-1' ribose proton line is now barely discernible.

After bubbling oxygen through the sample used for Figure 3A for 5 min, the photo-CIDNP spectrum (Figure 3B) reverted to that found previously in undegassed solution (Figure 1B).

Inspection of Table I reveals that the  $NAD^+$  spectrum without oxygen (Figure 3A) corresponds more closely to the calculated hfc of  $NAD\cdot$  than those of  $NADH^+$ . At longer delays in degassed solution  $NAD^+$  becomes stronger with respect to NADH and the relative  $NAD^+$  intensities show patterns intermediate between those of Figure 3A ( $NAD\cdot$  derived) and Figure 3B ( $NADH^+$  derived) as shown in Figure 4; the growth of the  $NAD^+$  lines occurs over a period of  $\sim 1$  ms. During this time no change occurs in the NADH signals.

These results are consistent with a primary electron-transfer step (eq 4) giving a radical ion pair as well as some involvement of the neutral radical pair,  $NAD\cdot$ -FH $\cdot$ . In oxygenated solutions the latter is ineffective as a source of  $NAD^+$  polarization which comes mostly from reactions 4, 8, and 9 with  $O_2$  as the electron acceptor in eq 9. In oxygen-free solution, however, only polarization arising from recombination reactions, of both radical pairs, is observed, giving different CIDNP patterns for  $NAD^+$ . These processes are discussed further in section VII.

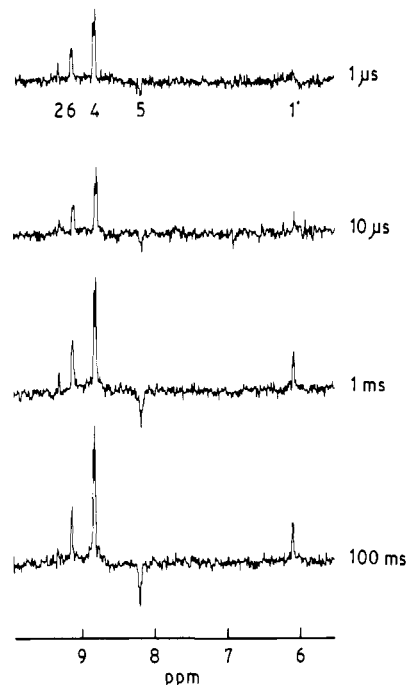


Figure 4. Photo-CIDNP spectra of  $\beta$ -NADH + flavin I in  $D_2O$ ,  $N_2$ -saturated solution, with delays as shown (other conditions as for Figure 1B).

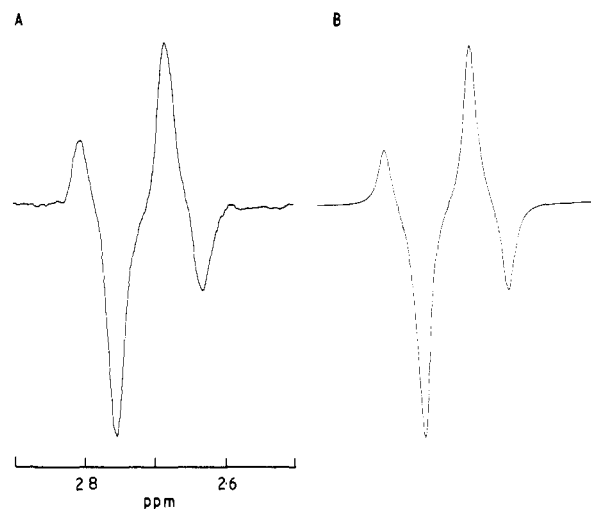


Figure 5. (A) Partial photo-CIDNP spectrum of  $\beta$ -NADH + flavin I in  $D_2O$ , 10- $\mu$ s delay, 1- $\mu$ s rf pulse (other conditions as for Figure 1B). (B) Computer simulation,  $A(4a) = 46.8$  G,  $A(4b) = 45.8$  G,  $\Delta g = -0.000222$ .

### VI. CIDNP Spectrum Simulation

Further information on the  $NADH^+$  radical cation is available from simulation of CIDNP intensities using the simple diffusion model proposed by Adrian.<sup>19</sup> We have chosen to focus on the C-4 protons of NADH partly for simplicity and partly because their striking multiplet CIDNP effect should give a good estimate of the  $g$  value of  $NADH^+$ . As the hfc's of these two protons are probably much larger than those of all other protons in the  $NADH^+\cdot$ - $F\cdot$  radical pair (see Table I and ref 20), it is possible to neglect the latter without introducing significant error. Optimum agreement between the line intensities measured from Figure 5A and those calculated for a two-photon radical pair was obtained by a least-squares minimization procedure and gave the following results:

(19) Adrian, F. J. *J. Chem. Phys.* **1970**, *53*, 3374; **1971**, *54*, 3912.

(20) Ehrenberg, A.; Müller, F.; Hemmerich, P. *Eur. J. Biochem.* **1967**, *2*, 286.

$$A(4a)/\Delta g = -2.11 \times 10^5 \text{ G} \quad (10a)$$

$$A(4b)/\Delta g = -2.06 \times 10^5 \text{ G} \quad (10b)$$

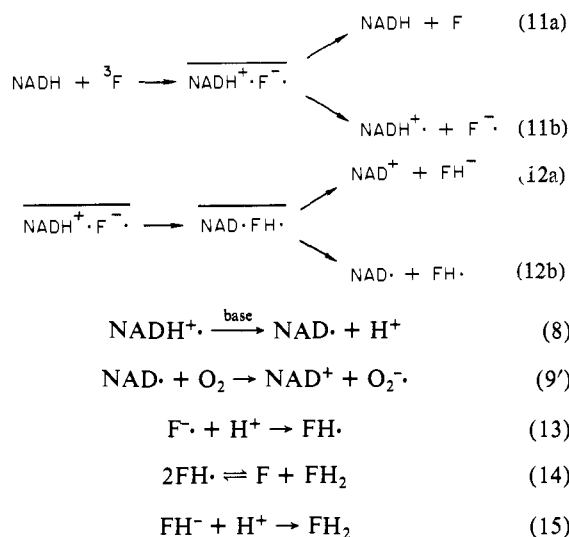
where  $A(4a)$  and  $A(4b)$  are the hfc's of the C-4 protons of NADH at 2.85 and 2.63 ppm, respectively, and  $\Delta g = g(\text{NADH}^{\cdot-}) - g(\text{F}^{\cdot-})$ . A partial spectrum calculated with these parameters is given in Figure 5B.

Assuming the mean of  $A(4a)$  and  $A(4b)$  to be 46 G (Table I), one obtains  $\Delta g = -0.0002$ , and, if<sup>21</sup>  $g(\text{F}^{\cdot-}) = 2.0034$ , then  $g(\text{NADH}^{\cdot-}) = 2.0032$ .

Using this  $g$  value difference and  $A(4a)$ ,  $A(4b)$  from eq (10a,b), computer simulations of the complete CIDNP spectrum (Figure 1B) were attempted. Good agreement was obtained (Figure 1D) with  $A(5) = -6.2$  G,  $A(1') = 5.0$  G, but with the remaining hyperfine couplings slightly smaller values than in Table I were found:  $A(2) = 1.0$  G,  $A(6) = 1.5$  G.

## VII. Discussion

The above observations of the NADH-flavin photoreaction are consistent with the following scheme in which the primary photochemical step is electron transfer.



The radical ion pair so formed can undergo back electron transfer, diffuse apart to give free radicals, or suffer proton transfer giving a pair of neutral radicals. This secondary pair either separates or reacts by forward electron transfer. Both radical pairs are sufficiently long lived to generate CIDNP. These events are followed by (de)protonations, oxidation of  $\text{NAD}^{\cdot}$  by  $\text{O}_2$ , and a termination reaction, presumably eq 14. The horizontal bars in eq 11 and 12 denote spin correlated radical pairs.

In fact, the photo-CIDNP results represented above are not sufficient to exclude the possibility of two parallel primary steps, i.e., electron and hydrogen-atom transfer, reactions 3 and 4, between triplet flavin and NADH. Our conclusions about the role of oxygen (see below) and the occurrence of electron transfer as a primary step are not affected by this, but we are unable to say whether the neutral pair  $\overline{\text{NAD}^{\cdot} \cdot \text{FH}^{\cdot}}$  is formed directly from  ${}^3\text{F}$  or indirectly via the radical ion pair.<sup>22</sup>

In the absence of oxygen, radicals which escape their geminate pairs (reactions 11b and 12b) are long lived, their polarizations

decaying by spin-lattice relaxation prior to further reaction. The CIDNP effects in Figure 3A thus arise from geminate radical-pair recombination and reflect the magnetic parameters of the radicals involved:  $\text{NAD}^{\cdot}$  in the case of  $\text{NAD}^+$  (eq 12b) and  $\text{NADH}^{\cdot+}$  in the case of  $\text{NADH}$  (eq 11b).

When oxygen is present, however, radicals not undergoing geminate reactions are rapidly oxidized (eq 9') without having time to relax, so transferring their polarization to the oxidation product,  $\text{NAD}^+$ . This is quite feasible: a diffusion-controlled reaction with the  $\sim 0.25$  mM  $\text{O}_2$  present in water at atmospheric pressure could easily cause the lifetimes of the radicals to be considerably shorter than their nuclear  $T_1$ 's (usually in the range  $10 \mu\text{s}$ – $10 \text{ms}$ ).<sup>24</sup> Similarly a rapid oxidation of  $\text{NAD}^{\cdot}$  would explain our failure to observe the kinetics of  $\text{NAD}^+$  formation.<sup>25</sup>

Now, since the part of the total reaction proceeding via the neutral radical pair has identical escape and recombination products ( $\text{NAD}^+$ ), a rapid reaction (eq 9') will cause destruction of the geminate  $\text{NAD}^+$  polarization arising from reaction 12a.<sup>10,27</sup> In other words, the polarizations of  $\text{NAD}^{\cdot}$  in eq 12b, and hence of  $\text{NAD}^+$  in eq 9', are equal in amplitude but opposite in phase to those of  $\text{NAD}^+$  in eq 12a and therefore tend to cancel, under aerobic conditions.

However, another route for the production of polarized  $\text{NAD}^+$  opens up when  $\text{O}_2$  is present, namely, eq 11b followed by eq 8 and 9'. No cancellation occurs here since the escape ( $\text{NAD}^+$ ) and recombination ( $\text{NADH}$ ) products of the electron-transfer pair (eq 11) are chemically distinct. Thus the  $\text{NAD}^+$  polarization becomes escape type characteristic of  $\text{NAD}^+$ .

The gradual changeover from recombined  $\text{NAD}^{\cdot}$  type polarization to escape  $\text{NADH}^{\cdot+}$  type for  $\text{NAD}^+$  in degassed solutions (Figure 4) is probably caused by slow oxidation of  $\text{NAD}^{\cdot}$  either by residual  $\text{O}_2$  or by flavin itself. The differences between Figures 1B and 3B, notably the relative strengths of the C-2 and C-6  $\text{NAD}^+$  proton signals, are most likely due to a small CIDNP contribution from the neutral radical pair, in Figure 1B, which is absent in  $\text{O}_2$ -saturated solution because of more complete cancellation.

The absence of a CIDNP signal from the C-1' ribose proton in  $\alpha$ - and  $\beta$ -NADH and NMNH remains puzzling. In aerobic conditions where both  $\text{NAD}^+$  and  $\text{NADH}$  CIDNP effects are derived predominantly from the same radical pair containing  $\text{NADH}^{\cdot+}$ , it is certainly surprising to find a proton enhanced in the escape product but not in the recombination product. We are unable to offer a convincing explanation of this result. The non-appearance of this line in Figure 3A can be attributed to a small hfc in  $\text{NAD}^{\cdot}$ .

The complete failure to detect CIDNP from either flavin itself or its reduced form,  $\text{FH}_2$ , is probably due to severe line broadening brought about by the equilibrium of eq 14. The fact that polarization of flavin I is often observed in its photoreaction with amino acids and proteins<sup>13</sup> no doubt reflects the much lower concentrations of  $\text{FH}_2$  produced in these reactions which are predominantly cyclic.

Although in principle possible, no change in the relative intensities of the NADH C-4 proton multiplet lines was found in the period  $1 \mu\text{s}$ – $100 \text{ms}$ . Schäublin et al.<sup>28</sup> have shown that the components of a strongly coupled AB multiplet should oscillate in a pulse experiment at a frequency related to the  $J$  coupling and the chemical shift difference. However, since the hfc of the two protons involved are rather similar (eq 10), the amplitude of oscillation should be very small.

Finally, simulation of the C-4 multiplet of NADH yields slightly different values for the hyperfine couplings of the two protons:

(21) Ehrenberg, A.; Eriksson, L. E. G.; Müller, F. In "Flavins and Flavoproteins"; Slater, E. C., Ed.; Elsevier: Amsterdam, 1966; p 44.

(22) Investigating the photochemistry of *p*-benzoquinone in the presence of triethylamine, Roth and co-workers<sup>23</sup> observed CIDNP in a reaction product (an enamine) characteristic of both cationic and neutral amine-derived radicals. They were able to reject the occurrence of two parallel reactions in favor of a stepwise mechanism on the grounds that the direct formation of the enamine from an amine cation radical would be chemically unreasonable. No such discrimination is possible here where the product,  $\text{NAD}^+$ , can be derived equally plausibly from both  $\text{NADH}^{\cdot+}$  and  $\text{NAD}^{\cdot}$ .

(23) Roth, H. D. In ref 12, Chapter 4.

(24) (a) Walling, C.; Lepley, A. R. *J. Am. Chem. Soc.* **1972**, *94*, 2007. (b) Closs, G. L.; Trifunac, A. D. *Ibid.* **1970**, *92*, 7227. (c) Closs, G. L.; Paulson, D. R. **1970**, *92*, 7229.

(25) The rate constant of reaction 9' is  $2 \times 10^9 \text{ M}^{-1} \text{ s}^{-1}$ .

(26) (a) Willson, R. L. *Chem. Commun.* **1970**, 1005. (b) Land, E. J.; Swallow, A. J. *Biochim. Biophys. Acta* **1971**, *234*, 34.

(27) Closs, G. L. *Chem. Phys. Lett.* **1975**, *32*, 277.

(28) Schäublin, S.; Höhener, A.; Ernst, R. R. *J. Magn. Reson.* **1974**, *13*, 196.

$A(4a) = 46.8$  G,  $A(4b) = 45.8$ , given the assumptions in section V. Although this difference is small (2%), we believe it to be real. Analyses of NADH spectra obtained with other dyes give similar results.<sup>29</sup> A slightly nonplanar geometry of the nicotinamide ring in NADH<sup>+</sup>, brought about by a stacking interaction with the adenine ring could be responsible.

(29) Hore, P. J.; Kaptein, R., unpublished results.

**Acknowledgment.** This work was performed at the national NMR facility at the University of Groningen, supported by the Netherlands Foundation for Chemical Research (S.O.N.) with financial aid from the Netherlands Organization for the Advancement of Pure Research (Z.W.O.). P.J.H. is grateful to the Royal Society, London, for the award of a research fellowship.

**Registry No.** NADH, 58-68-4; 7,8,10-trimethyl-3-carboxymethylisoxalazine, 20227-26-3.

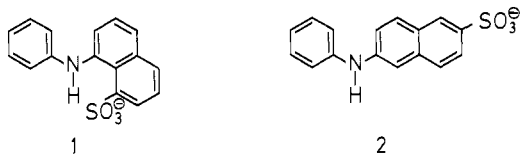
## Reactivity and Decay Pathways of Photoexcited Anilinonaphthalenes

K. H. Grellmann\* and U. Schmitt

Contribution from the Max-Planck-Institut für biophysikalische Chemie, Abteilung Spektroskopie, D 3400 Göttingen, West Germany. Received March 1, 1982

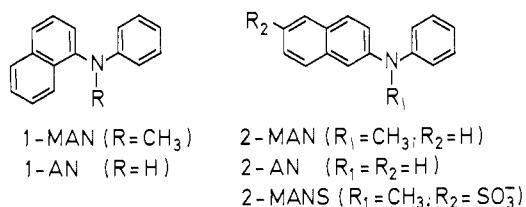
**Abstract:** *N*-Methyl-2-anilinonaphthalene (**2-MAN**) is converted by light into 7-methyl-7*H*-benzo[*c*]carbazole (**7-MBC**) and 5-methyl-6,7-dihydro-5*H*-benzo[*c*]carbazole (**9**). The reaction takes place only in the absence of oxygen and is regioselective; i.e., the isomeric 5-methyl-5*H*-benzo[*b*]carbazole (**5-MBC**) is not formed. Ring closure takes place from the excited triplet state of **2-MAN** and a zwitterionic intermediate was found in flash experiments. *N*-Methyl-2-anilino-6-naphthalenesulfonate (**2-MANS**) behaves similarly. Caution should therefore be exercised if such compounds are used as fluorescence probes. *N*-Methyl-1-anilinonaphthalene (**1-MAN**) is photochemically more stable than **2-MAN**.

Anilinonaphthalenes, e.g., **1** and **2**, have been widely used as



fluorescence probes for structure studies in biochemistry<sup>1</sup> because the quantum yield and the spectral distribution of the fluorescence of such compounds depend strongly on solvent polarity.

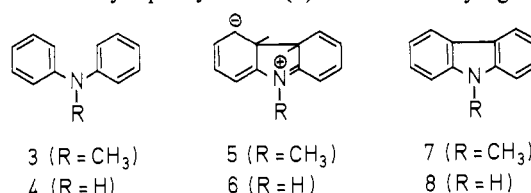
Since diphenylamines are by light effectively converted into carbazoles,<sup>2</sup> it is to be expected that anilinonaphthalenes undergo similar photoinduced ring-closure reactions forming benzo-carbazoles. Such photoproducts which strongly fluoresce could cause artifacts if the parent compounds are used as fluorescence labels. We therefore investigated the photochemical properties of *N*-methyl-1-anilinonaphthalene (**1-MAN**) and *N*-methyl-2-



anilinonaphthalene (**2-MAN**) in some detail by means of steady-state and flash experiments. Similar to **1** and **2** the fluorescence spectra and the fluorescence quantum yields of **1-**

**MAN** and **2-MAN** depend strongly on solvent polarity.

We began our studies with the *N*-methyl compounds in order to avoid complications due to side reactions which were observed in the case of diphenylamines. For instance, in the presence of oxygen *N*-methyl-diphenylamine (**3**) is converted by light<sup>3</sup> into



*N*-methylcarbazole (**7**) via the zwitterionic dihydrocarbazole intermediate<sup>4</sup> **5**. In the case of **4** side reactions occur<sup>5</sup> due to hydrogen abstraction from the N-H group of the corresponding zwitterion **6**, which reduce the quantum yield of the formation of **8**.

### Results

***N*-Methyl-2-anilinonaphthalene (2-MAN). Steady-State Photochemistry and Product Analysis.** Illumination of degassed solutions of **2-MAN** in acetonitrile, ethanol, or methylcyclohexane (MCH) results in the formation of 7-methyl-7*H*-benzo[*c*]carbazole (**7-MBC**) and 5-methyl-6,7-dihydro-5*H*-benzo[*c*]carbazole (**9**) with a total quantum yield of 5–10%. The concentration ratio **7-MBC**:**9** is about 2:1. Both compounds were identified by comparison with authentic samples (mp, UV and NMR spectra). The UV spectra of **2-MAN** before and after illumination together with the spectrum of **7-MBC**, all in acetonitrile, are given in Figure 1. In MCH the absorption spectrum of **7-MBC** is similar to that in acetonitrile but the absorption peaks between 350 and 370 nm

(1) (a) Radda, G. K. *Curr. Top. Bioenerg.* **1971**, *4*, 81–126. (b) Brand, L.; Gohlke, J. R. *Annu. Rev. Biochem.* **1972**, *41*, 843–68. (c) Radda, G. K.; Vanderkooi, J. *Biochim. Biophys. Acta* **1972**, *265*, 509–49. (d) Träuble, H. *Biomembranes* **1972**, *3*, 197–227. (e) Azzi, A. *Q. Rev. Biophys.* **1975**, *8*, 237–316.

(2) (a) Parker, C. A.; Barnes, W. J. *Analyst (London)* **1957**, *82*, 606–18. (b) Bowen, E. J.; Eland, J. H. D. *Proc. Chem. Soc., London* **1963**, 202. (c) Grellmann, K. H.; Sherman, G. M.; Linschitz, H. *J. Am. Chem. Soc.* **1963**, *85*, 1881–2.

(3) Fischer, G.; Fischer, E.; Grellmann, K. H.; Linschitz, H.; Temizer, A. *J. Am. Chem. Soc.* **1974**, *96*, 6267–9.

(4) (a) Förster, E. W.; Grellmann, K. H. *J. Am. Chem. Soc.* **1972**, *94*, 634–5. (b) Förster, E. W.; Grellmann, K. H. *Chem. Phys. Lett.* **1972**, *14*, 536–8. (c) Förster, E. W.; Grellmann, K. H.; Linschitz, H. *J. Am. Chem. Soc.* **1973**, *95*, 3108–15.

(5) Wolff, Th. Masters Thesis, University of Göttingen, Göttingen, West Germany, 1972.